Alignment requirements for the Advanced Virgo+ Arm cavity using the Green laser

VIR-1165A-19

Maddalena Mantovani[1*], Julia Casanueva[1], and Jonathan Brooks[1]

[1]*EGO - European Gravitational Observatory*

Date: November 15, 2019

[*] *corresponding author:*
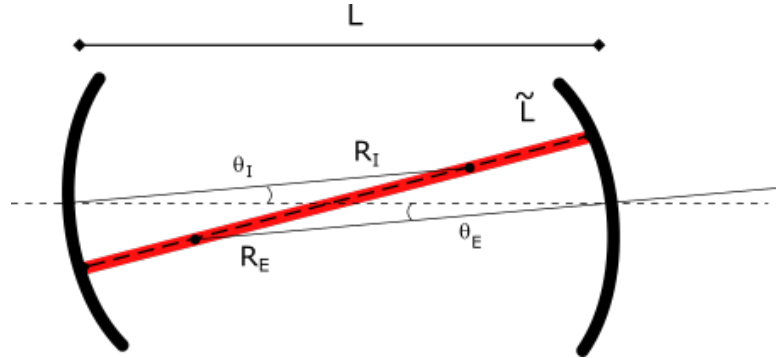
Contents

1   Introduction

Figure 1: Schematic drawing of a cavity axis displacement due to the cavity mirror misalignment. The cavity length due to the mirror misalignment is varied from L to $\tilde{L}$.

The main difference from the Advanced Virgo Plus optical configuration and the O3 configuration is the presence of the SR cavity. The lock acquisition will be completely different from the one used in the O2 and O3 observing runs [1]. The lock acquisition will rely on the use of auxiliary beams (with a green beam injected from the terminal benches) [3] [2].

A fundamental requirement to be set is the angular control accuracy needed for the long arm cavity when locking with the green laser.

If the mirrors or the beam in a cavity is misaligned the optical axis will be tilted/shifted having the beam axis which will lay on the line which crosses the mirrors center of curvature, see Figure 1.

A misalignment of the cavity axis generates two main effects. The first effect is the **optical path variation** due to the optical axis misalignment, the second effect is the **generation of Higher Order Modes (HOMs)**. The first effect, which is the dominant one in terms of cavity performance, is purely a geometrical effect, visible in Figure 1, having an optical path length variation equal to $\frac{\tilde{L}}{L}$. This variation on the cavity length can easily bring the cavity far from the working point (the resonant condition).

But, when a misalignment occurs in a locked cavity, the continuous servo loop restores the longitudinal working point, i.e. the resonance conditions, acting on the longitudinal position of one of the two cavity mirrors keeping the cavity length under control.

This compensation of the cavity length works up to the longitudinal control loop bandwidth, the loop unity gain frequency (u.g.f.). Above this frequency the cavity length is not controlled thus a misalignment could bring the optical system far from the optimal working point.

From the other hand the lock of the cavity can not prevent the generation of HOMs which will anyway spoils the cavity performance.

The second effect indeed, which is the generation of HOMs, has the main consequence of subtracting energy from the 00 mode reducing the intra-cavity power and the longitudinal error signal optical gain (slope at the working point). The reduction of the optical gain has a strong effect on the longitudinal control bringing the control toward the instability. The feedback loops are stable within certain thresholds of phase and gain margins, and a safe margin for the gain is usually smaller than a factor 2.
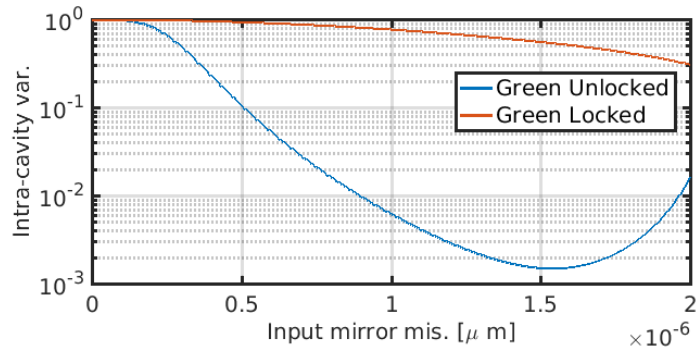
Figure 2: Comparison of the intra-cavity power drop, in percentage, for the Green beam in case of cavity locked or not locked. It is visible that the locking of the cavity makes the system much more robust against misalignments and the effect of the misalignment is reduced to the generation of HOMs, while in the first case the dominant effect is the increase of the optical path length.

Indeed, the effect of the lock of the cavity with respect to the un-locked cavity is visible in Figure 2, where the Intracavity power variation (in percentage) is plotted as a function of the Input misalignment. The power drop in case of a not locked cavity occurs for very small misalignment while if the locking is active, the cavity is more robust against misalignment. The power decrease visible in the red curve due to the misalignment, is due to the generation of HOMs which are not resonating in the long arm, which is the cause of the optical gain decrease in the longitudinal error signal.

Thus it can be concluded that the variation of the optical path due to misalignment counts above the U.G.F. of the longitudinal control loop, while the generation of HOMs counts more below the U.G.F..
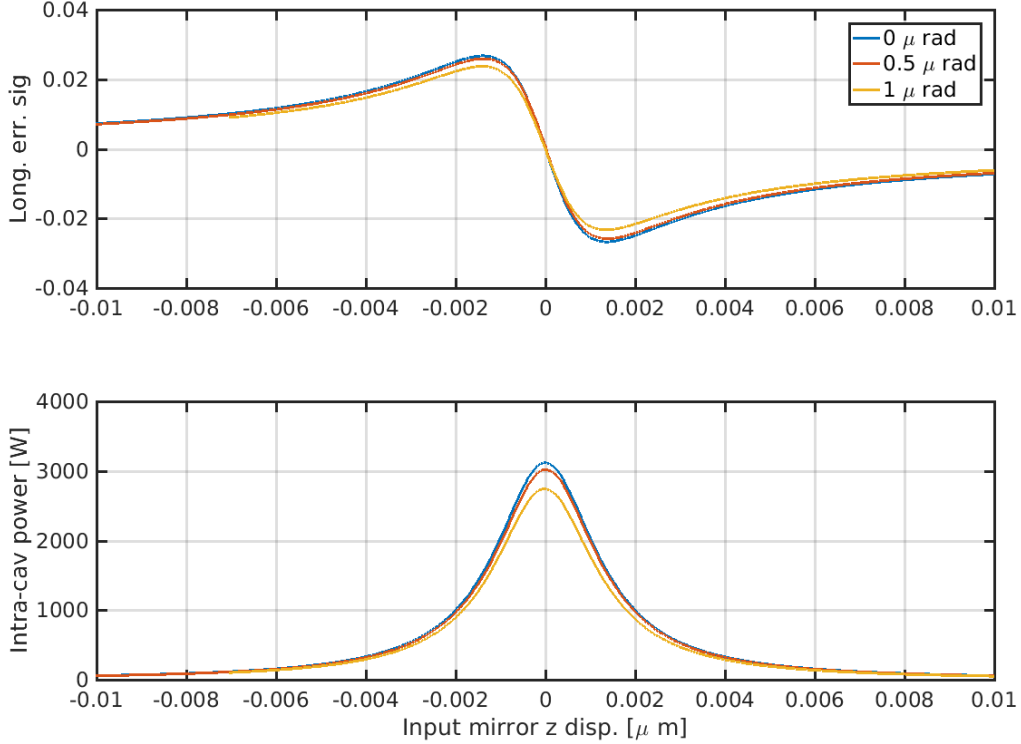
1.1 Generation of HOMs - below the U.G.F.

Figure 3: Effect of misalignments on the intra-cavity power and on the error signal shape for the Green cavity. The increase of optical path length has been compensated in the plot, for visual reasons, to have the optimal working point at 0. The main effects of the misalignment is the reduction of optical gain, slope of the error signal, and the loss of circulating power.

As it has been described in the introduction, in a locked cavity the effect of a misalignment is the generation of HOMs (01 and 10 depending on the misalignment direction) degrading the recycling of the power and the optical gain of the longitudinal error signal, see Figure 3. The amplitude of the $\text{TEM}_{01/10}$ ($\alpha_{01/10}$) generated for the a given misalignment depends on the cavity properties as:

$$\alpha_{01/10} \quad \propto \theta/\theta_{div} \tag{1.1}$$

$$\alpha_{01/10} \quad \propto x/w_0 \tag{1.2}$$

The first in case of tilt (θ) and the second in case of shift (x).
Where both the divergence angle (θ_{div}) and the waist size (w_0) depends on the laser wavelength.
It is interesting to compare then performance of the Advanced Virgo cavity, with the YAG beam which is well known in terms of commissioning, and the same cavity with the Green beam. Considering that the two beams have to matched to the same cavity (Advanced Virgo+ long arm cavity), the two Rayleigh ranges have to be the same:

$$z_{R_{Green}} \quad = \quad z_{R_{YAG}} \tag{1.3}$$

$$\frac{\pi w_{0_{Green}}^2}{\lambda_{Green}} \quad = \quad \frac{\pi w_{0_{YAG}}^2}{\lambda_{YAG}} \tag{1.4}$$

$$\tag{1.5}$$

knowing that $\lambda_{YAG} = 2\lambda_{Green}$, it can be written:

$$\frac{w_{0_{Green}}^2}{\lambda} = \frac{w_{0_{YAG}}^2}{2\lambda} \tag{1.6}$$

$$w_{0_{Green}} = \frac{1}{\sqrt{2}}w_{0_{YAG}} \tag{1.7}$$

the divergence angle can be written as a function of the waist size as:

$$\theta_{div} = \frac{\lambda}{\pi w_0} \tag{1.8}$$

$$\theta_{div_{Green}} = \frac{\frac{1}{2}\lambda_{YAG}}{\pi \frac{1}{\sqrt{2}}w_{0_{YAG}}} \tag{1.9}$$

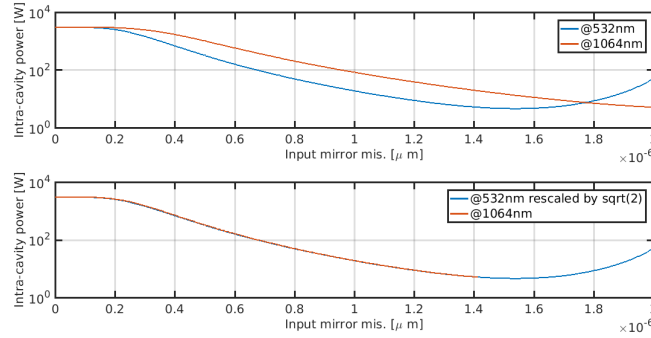$$\theta_{div_{Green}} = \frac{1}{\sqrt{2}}\theta_{div_{YAG}} \tag{1.10}$$

Figure 4: Comparison of the intra-cavity power drop, in percentage, for the YAG and Green lasers due to the generation of HOMs for the input mirror misalignment. It is visible that the effect for the Green cavity is a factor $\sqrt{2}$ stronger.

Thus:

$$\alpha_{01/10}\Big|_{Green} = \sqrt{2} \cdot \alpha_{01/10}\Big|_{YAG} \tag{1.11}$$

In this case the effect for the green is $\sqrt{2}$ stronger than for the YAG, see Figure 4.

1.2   Cavity optical path variation - above the U.G.F.

The variation of the cavity length due to the geometrical displacement of the beam axis has a stronger impact when the finesse is higher and the wavelength is lower since the optical path change has to be compared with the cavity linewidth $FWHM$ which is:

$$FWHM = \frac{\lambda}{4\mathcal{F}} \tag{1.12}$$

In a cavity which has a small FWHM it is easy to go far from the resonance region even for small misalignments. The variation of the optical path length can be written as [4]:

$$\frac{\tilde{L}}{L} \sim 1 + \frac{1}{2}\left(\frac{-g_E}{1 - g_I g_E}\right)\theta_I^2 + \frac{1}{2}\left(\frac{-g_I}{1 - g_I g_E}\right)\theta_E^2 + \left(\frac{1}{1 - g_I g_E}\right)\theta_I\theta_E \tag{1.13}$$

Where $\tilde{L}$ is the length variation, $g_{I/E}$ are the stability parameters ($g_i = 1 - L/R_i$), and θ_i is the i-mirror misalignment.

This optical path change would not affect the cavity behavior if the longitudinal control had an infinite accuracy and control bandwidth, keeping the cavity locked at all the frequencies. In reality it is not the case, thus this will set a maximum mirror (or beam) allowable misalignment, which will depend on the frequency since the effect of the longitudinal loop has to be taken into account.
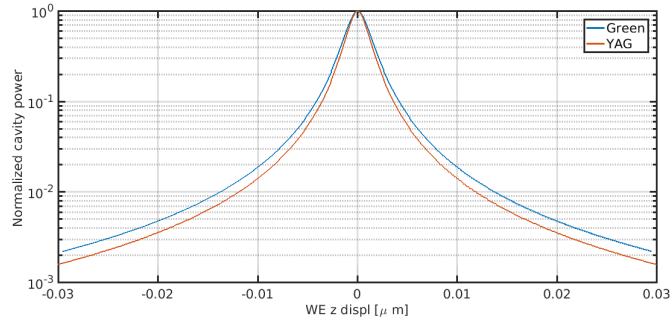

Figure 5: Comparison of the normalized intra cavity power in case of Green and YAG lasers. It is visible that the difference is very small (about 1.18 between the two curves) and it is due to the small difference in Finesse and the factor 2 in FSRs.

Considering this geometrical effect the Advanced Virgo+ cavities, using the green or the YAG beam, are almost equivalent (having a FWHM difference of 1.18).

Indeed the coating of the arm cavity mirrors has been chosen to have a finesse for the Green beam to be about a factor 2.35 smaller than the YAG beam. However considering that the wavelength of the YAG is the double of the Green (1064nm with respect to 532nm) the requirements, considering only this mechanism, on the alignment will scale as the ratio of the FWHM (the YAG requirements are 1.18 times more stringent than the Green cavity), see Figure 5. The fact that this mechanism is the dominant one does not mean that the requirements on the YAG cavity above the U.G.F. will be smaller of 1.18 times with respect to the green, since the generation of HOMs will contribute too, see Section B.

Then in the following the two main requirement principles which are considered are:

- The angular accuracy needed to have a maximum optical gain variation of 10% (within the longitudinal control bandwidth) to maintain the lock [1].

- The angular accuracy needed to have the cavity locked, above the longitudinal control bandwidth, having the maximum allowable power loss of 10% which corresponds to a longitudinal displacement within $\sim 1/3$ of the FWHM. This ensure the cavity to be more or less in the working position maintaining a small circulating power variation, to keep a good performance of the cavity [2].

It is worth to mention that for this analysis the linear region taken into account is the one of the simple error signal, not of the normalized one which would have increased strongly the linear region, see D. This choice has been done since the use of the normalized error signal will increase the robustness of the lock but it will not improve the cavity performance (i.e. the amount of circulating power).

After the requirements on the mirror cavity angular displacement is obtained, this computation can be used also to set the requirement on the maximum allowable green beam jitter, to be given as input to the ALS

---

[1]The factor two has been chosen knowing that the typical maximum gain margin of the longitudinal control filters is usually smallre than a factor 2. Thus in order to maintain the good performance of the cavity the requirement the optical gain variation has to be well below the gain margin.

[2]It has be considered that the 10% requirement is for lock acquisition while for the since mode the requirement is 0.1% of cavity power variation [5].

Advanced Virgo+ subsystem to design a Beam Pointing Control system (BPC system [7]). For the Green beam jitter requirements it has to considered that a further constrain will be given by the robustness of the CITF lock versus the angular displacement of the Input mirrors (which will follow the green beam thanks to the drift control of the arm cavities). This computation is presently on-going [6].
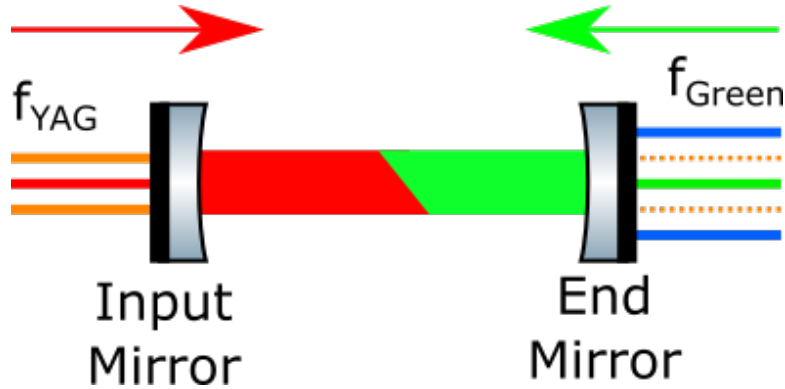
2 Cavity modeling

Figure 6: Schematic of the Advanced Virgo+ arm cavity. The red beam is the YAG beam (1064 nm) while the Green is the 532 nm. The sidebands considered from now on are only the 6 MHz, orange lines for the YAG cavity lock, and the 37 kHz, blue lines for the Green cavity lock, both are not resonating in the arm cavity. The longitudinal photo-diode is placed in transmission of the arm cavity for the YAG beam (since the YAG beam is injected from the Input mirror side) and in reflection from the cavity for the green (since the Green beam is injected from the End mirror side).

The single cavity, see Figure 6, has been modeled using the modal simulation tool *Finesse* [8] using as optical parameters the ones listed in Table 1.

Parameter	Value	Parameter	Value
T_{NI} for YAG	1.377%	T_{NI} for Green	1.01%
T_{NE} for YAG	4.4 ppm	T_{NE} for Green	2.9%
T_{WI} for YAG	1.375%	T_{WI} for Green	1.01%
T_{WE} for YAG	4.3 ppm	T_{WE} for Green	2.2%

Table 1: Optical parameters of the Advanced Virgo+ in case if YAG or Green laser is used. It is worth to be mentioned that, in the following analysis, the parameters from the WE cavity will be used, since they are more challenging for the accuracy requirements (2.2% of transmission instead of 2.9% of the NE mirror).

It is worth to be mentioned that, in the following analysis, the parameters from the WE cavity will be used, since they are more challenging for the accuracy requirements (2.2% of transmission instead of 2.9% of the NE mirror).

The *Finesse* file used for the simulations is visible in appendix E.

3 Accuracy requirement within the longitudinal control bandwidth - optical gain variation

As it has been described in the previous section, within the frequency band of the longitudinal control, the first order effect on the optical path due to the geometrical variation of the cavity length can be neglected since an active servo-loop is used to keep the cavity in the working point (on its resonance).

The implementation of the lock in the simulation is fundamental for the computation of the low frequency angular accuracy requirements since the real conditions have to be reproduced.

In the following a control bandwidth of about 1MHz, since these cavities will be locked acting on the laser, has been considered. A study on the needed control accuracy to obtain reliable results, for the simulation outcomes, is described in Appendix C.

For the frequency region below the U.G.F., as it has been described before, the misalignment requirements are set in order to have a maximum optical variation of a factor 0.1, since the gain margin of the typical loop is usually smaller than a factor 2, at maximum. The optical gain is defined as the low frequency limit of the Transfer Function between the mirror z displacement and the photo-diode response $TF\left(\frac{s_i}{z}\right)$ which is essentially the slope of the error signal in its linear region.

3.1 Arm cavity locking

In order to lock the error signal has to be generated, for this reason a phase modulation of 37kHz, with a modulation index of 0.15 which value is not relevant for this analysis since no longitudinal control noise evaluations have been performed, has been added to the carrier field and the error signal has been detected in reflection to the cavity, at the B8 detection port, since the green beam injection occurs at the terminal mirror. While for the YAG beam the injection is at the input mirror
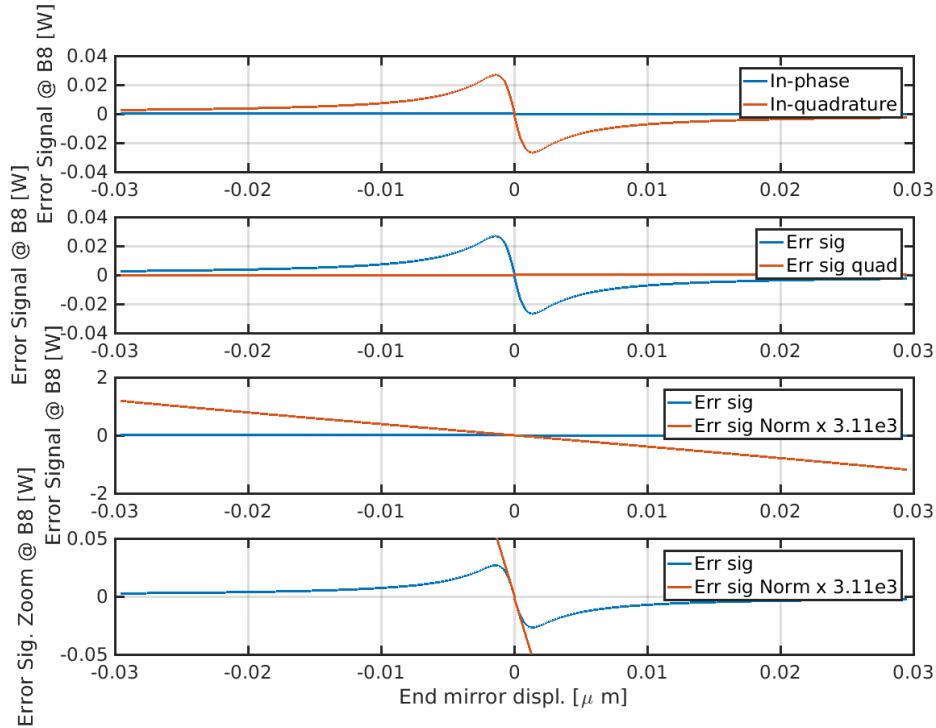
Figure 7: *1st plot from the top:* The in-phase and quadrature signal of the reflected beam (B8), blue and red curve respectively. *2nd plot:* The error signal, blue curve, and its quadrature, red curve. For convention the demodulation phase is tuned to have all the signal in the In-phase quadrature, blue curve. *3rd plot:* Comparison between the error signal and the normalized signal, on the intra-cavity power. It is visible that using the normalized error signal the linear region become very wide. *4th plot:* Zoom of the comparison between the error signal and the normalized signal, on the intra-cavity power.

The signal used for the lock is visible in the second plot of Figure 7, after the demodulation phase tuning to have the signal in the In-phase quadrature.
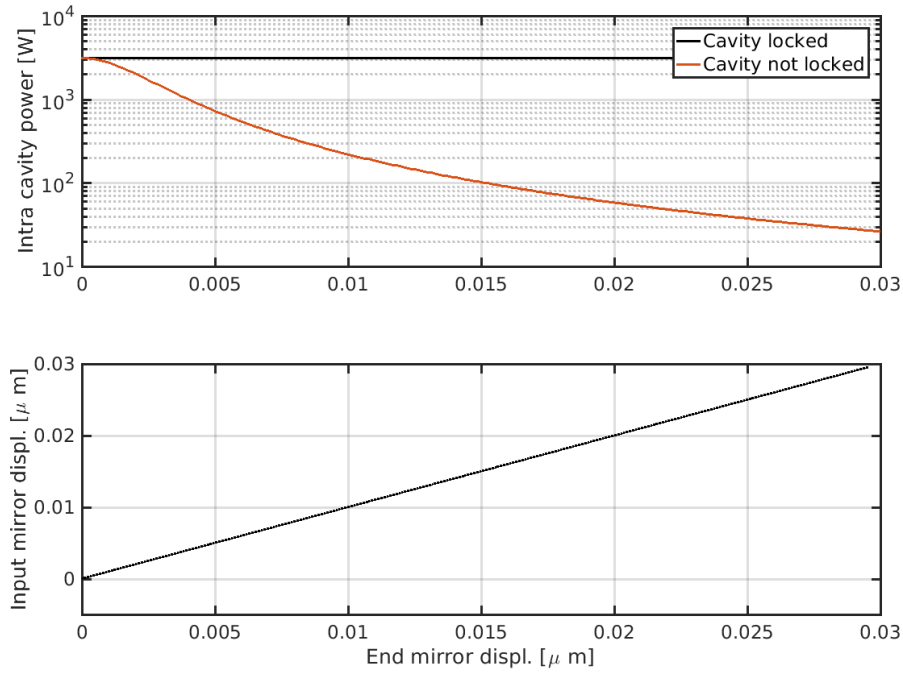
Figure 8: Effect of the lock on the green cavity while the End mirror is displaced in the longitudinal direction. It is visible that the lock compensates the mirror displacement acting on the Input mirror keeping the cavity on resonance.

The effect of the lock of the cavity is visible in Figure 8.

3.2   Simulation and Results

In order to compute the requirements on the optical gain variation the angular position of the two cavity mirrors has been scanned between $-1.1 \mu rad$ and $1.1 \mu rad$ and the optical gain at the working point has been measured. The working point along z is where the longitudinal error signal crosses zero and the recycling power is at its maximum, see Figure 3. When a misalignment occurs, due to the generation of HOMs, the optical gain decreases.

Of course there are mirror misalignment combinations, for instance the ones that make the optical axis to be shifted, that are less affecting the cavity performance but since the two mirror alignment are un-correlated the requirement on the mirror misalignment is set to be equal to the radius of the circle inside which the optical gain variation is smaller than 0.9.
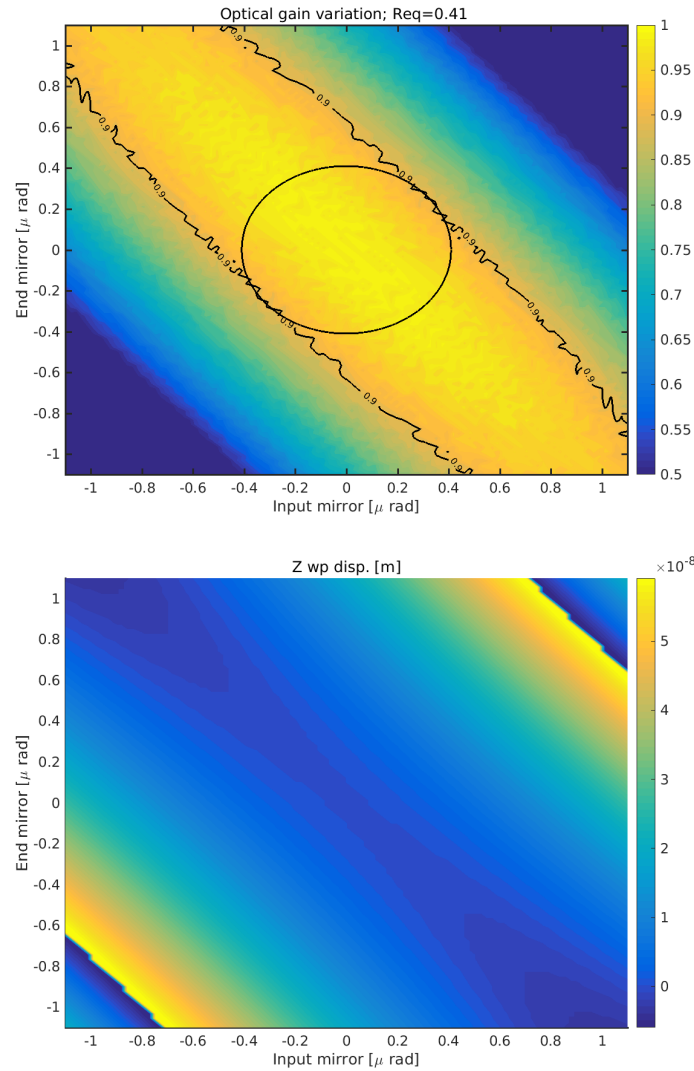
Figure 9: **Top Plot:** 3D plot of the optical gain variation for the longitudinal error signal, the requirement is set to have an optical gain variation between 0.9 to 1. The requirement on the mirrors misalignment, within the locking control bandwidth, become then 0.41 $\mu rad\ ToT_{RMS}$. **Bottom Plot:** Mirror displacement along z to keep the cavity locked.

From the simulation the maximum allowable mirror misalignment is 0.41 μrad, see top plot of Figure 9.

4   Angular requirements above the longitudinal control bandwidth - optical path increase

In order to set the requirements above the longitudinal control U.G.F. the mirrors misalignment have been scanned without applying the lock and the intracavity power variation has been computed. Essentially the intra-cavity power at the 0 longitudinal position, of Figure 10, for a misaligned cavity is compared with the aligned one. The Requirement is set in order to have a power loss of maximum 10% which corresponds to the region highlighted with the dashed red lines.
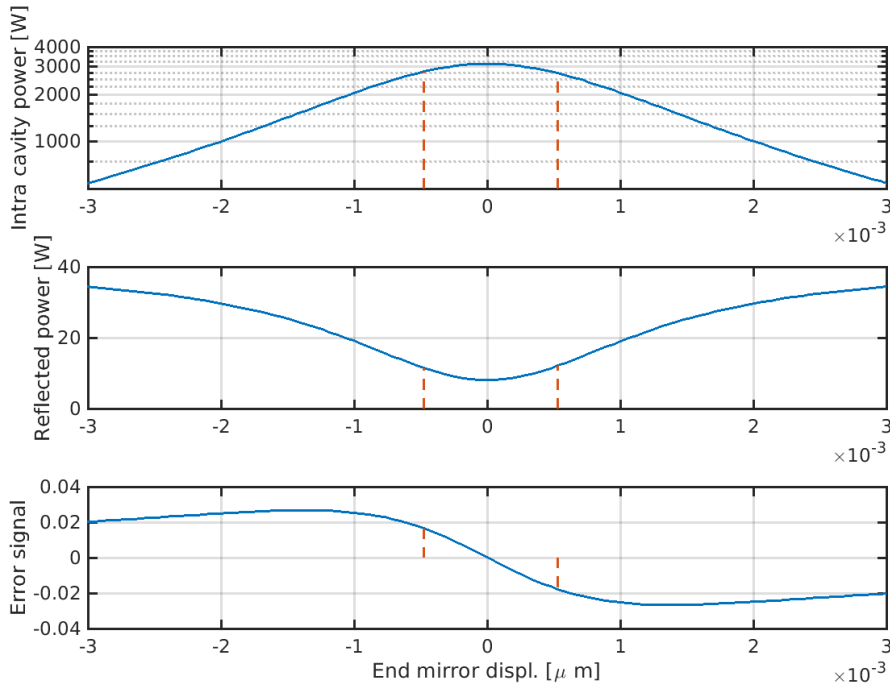The result is visible in Figure 11.

Figure 10: *Top plot:* Scan of the intra-cavity power as a function of the End mirror displacement. The dashed red lines highlight the safety region, for which the requirements have been set. The minimum allowable power drop corresponds then to have an intra-cavity power of 2799 W (a loss of $\sim 10\%$ having a safety region of about $1/3$ of the FWHM, i.e. $\pm 4.729 \cdot 10^{-4} \mu m$ with respect to $FWHM = 1.4 \cdot 10^{-3} \mu m$). *Middle plot:* Scan of the reflected power. *Bottom plot:* Scan of the locking error signal as a function of the End mirror displacement, on which the requirement has been computed.

As it is visible in Figure 2 the first order effect which makes the cavity to go out of resonance due to a misalignment is the fact that the misalignment increases the optical path length, as it is computed in section 1.2. If the longitudinal control can not compensate it, due to the fact that the misalignment occurs in a range of frequency above the loop UGF, the cavity can easily loose the resonance condition.

Thus the requirements in this frequency region can be set in order to have the cavity in resonance having a maximum power drop of 10%, which corresponds for the Green cavity (with 40 W of input power) to a minimum circulating power of 2.8kW, see Figure 10.
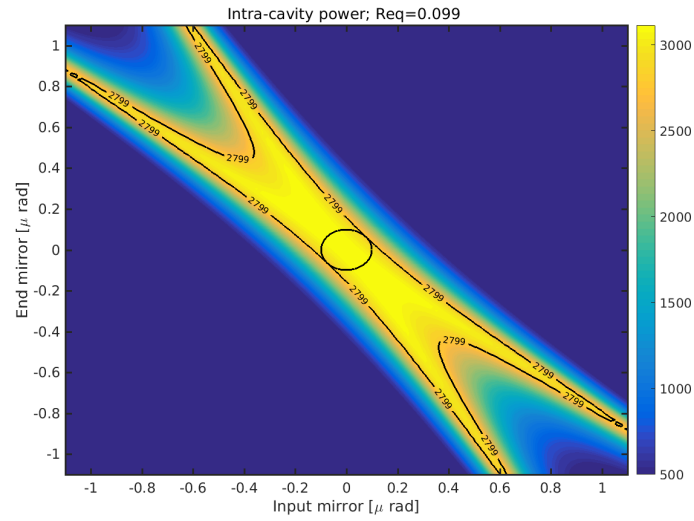
Figure 11: 3D plot of the intra-cavity power as a function of the mirror misalignment. The requirement on the mirrors misalignment, within the locking control bandwidth, become then 0.099 $\mu rad \sqrt{Hz}$.

The intra-cavity power has been plotted as a function of the mirror angular displacements, see Figure 11. The circle in Figure 11 highlights the maximum un-correlated displacement of the mirrors in order to have the longitudinal error signal well within the linear region which corresponds to $\sim 0.1\ \mu rad/\sqrt{Hz}$.

4.1   Green cavity mirror angular accuracy requirements

The requirements obtained in sections 3.2 and 4 can be summarized in Table 2.

Frequency region	Requirement value
below Arm lock UGF	0.41 [μrad ToTrms]
well above Arm lock UGF	0.099 [$\mu rad/\sqrt{Hz}$]

Table 2: Angular displacement requirements for the Advanced Virgo+ cavity mirrors using green beam.

Moreover the overall requirement, as a function of the frequency, is plotted in Figure 12 using a lock UGF of 1kHz.
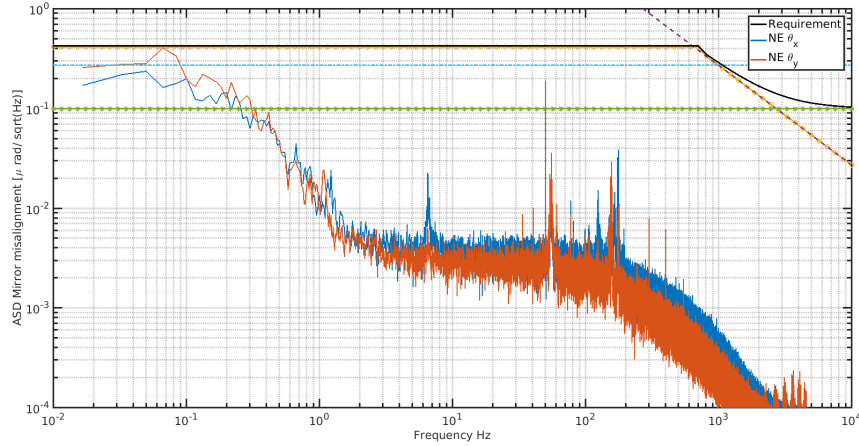
Figure 12: Spectra of the mirror angular requirements for the cavity mirrors as a function of the frequency. The lock UGF has been set for this computation at 1kHz. The End cavity mirror angular displacement ASD, in pitch and yaw respectively, has been plotted to give an idea of the typical mirror angular displacement.

In order to have the two requirement in function of the frequency the effect of the lock has been considered. The requirement shown in Figure 12, are computed as the following:

- the requirement below the U.G.F. are shown in the yellow dashed-circle line, in which the requirement is constant at $0.41\mu rad$ up to the crossing with the $1/f$ curve (the simple integrator). The gain of the integrator is set to have at 1kHz the misalignment which correspond to a loss of the circulating power of a factor 0.05, light blue dashed curve;

- for the requirement above the U.G.F. the lock does not have to be taken into account thus the requirement is a flat line at $0.099\mu rad/\sqrt{Hz}$, green dashed-starred line;

- the total requirement, black curve, is the incoherent sum of the two contributions.

In order to have an idea of the typical mirror displacement an ASD (Amplitude Spectral Density) of the cavity mirror angular displacements, in θ_x/y which correspond to pitch and yaw respectively, is plotted on top of it. The typical accuracy requirement for the cavity mirror controlled using the Drift control is about few tens of μrad, which results to be compliant with the accuracy requirement in case of lock with the Green beam [3]. By the way if the locking bandwidth will change significantly the spectral requirements have to be reviewed.

4.2 Angular requirements in the beam basis

In order to switch from the mirror modes, Input and End mirrors, to the beam modes, shift and tilt, a simple change of basis can be performed as in [9]:

$$\begin{pmatrix} \theta_b \\ x_b \end{pmatrix} = \begin{pmatrix} 1 & -\frac{R_E}{R_I} \\ 1 & \frac{R_E}{R_I} \end{pmatrix} \cdot \begin{pmatrix} \theta_I \\ \theta_E \end{pmatrix}$$

Where $\theta_{I/E}$ are the misalignment of the Input and End mirror respectively (considering the positive direction of the angle perpendicular to the HR face of the mirrors, the $R_{I/E}$ are the radius of curvature of the two mirrors, while the θ_b is the cavity beam misalignment and x_b is the cavity beam shift.

In order to set the requirements the shift and the tilt of the of the cavity axis has to be computed in physical units, such as mm for the beam shift and rad for the beam tilt.

---

[3]The control using the local controls, by means of optical levers connected to ground, has an accuracy which do not fulfill the requirements, which is few $\mu rad/h$.

$$\left(\begin{array}{c} \theta_b \big|_{rad} \\ x_b \big|_{mm} \end{array} \right) = \left(\begin{array}{cc} \alpha & -\alpha \frac{R_E}{R_I} \\ \beta & \beta \frac{R_E}{R_I} \end{array} \right) \cdot \left(\begin{array}{c} \theta_I \\ \theta_E \end{array} \right)$$

Thus in the following subsections the α and β calibration factors computation will be described.
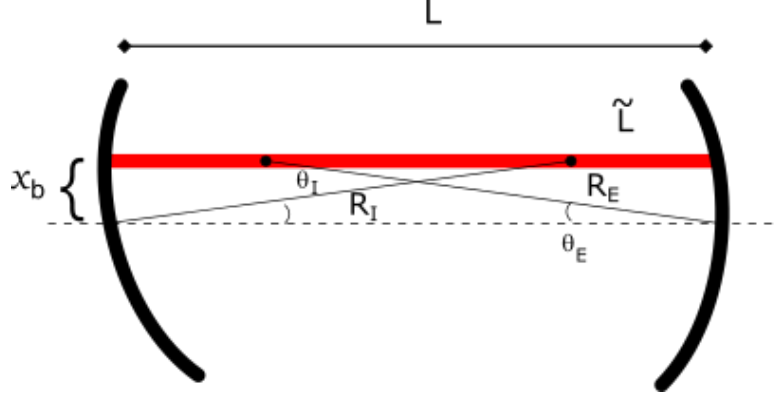
4.2.1 Beam shift calibration

Figure 13: Schematic drawing of a cavity axis shift due to the cavity mirror misalignment.

In order to compute the calibration factor for a pure shift, see Figure 13, in millimeters $x_b \big|_{mm}$ the condition of pure shift has to be applied:

$$\theta_b = 0 = \alpha \theta_I - \alpha \frac{R_E}{R_I} \theta_E \tag{4.1}$$

$$\theta_E = \frac{R_I}{R_E} \theta_E \tag{4.2}$$

$$\tag{4.3}$$

knowing geometrically that:

$$x_b \big|_{mm} = R_I/1000 \theta_I \tag{4.4}$$

it can be written, using Equations 4.3 4.4:

$$x_b \big|_{mm} = \beta \theta_I + \beta \frac{R_E}{R_I} \theta_E \tag{4.5}$$

$$R_I/1000 \cdot \theta_I = \beta \theta_I + \beta \theta_I \tag{4.6}$$

$$R_I/1000 \cdot \theta_I = 2\beta \theta_I \tag{4.7}$$

the factor 1000 is due to the fact that the calibration is in millimeters, thus obtaining

$$\beta = R_I/1000/2 = 0.71 \tag{4.8}$$
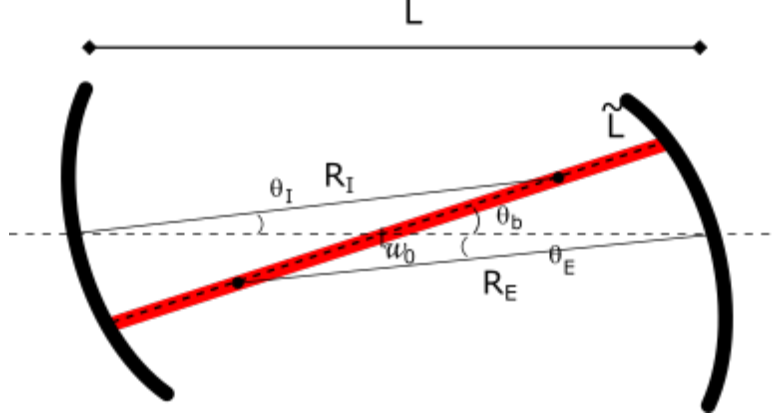
4.2.2 Beam tilt calibration

Figure 14: Schematic drawing of a cavity axis tilt due to the cavity mirror misalignment.

From the other hand imposing the pure tilt, see Figure 14

$$x_b = 0 = \beta\theta_I + \beta\frac{R_E}{R_I}\theta_E \tag{4.9}$$

$$\theta_E = -\frac{R_I}{R_E}\theta_I \tag{4.10}$$

considering that the cavity waist position, if the origin is at the input mirror, is at:

$$w_0\Big|_z = \frac{L + R_I - R_E}{2} \tag{4.11}$$

we can then compute $\theta_b\Big|_{rad}$ as:

$$\theta_b\Big|_{rad} = \frac{\theta_I R_I}{R_I - \frac{L + R_I - R_E}{2}} \tag{4.12}$$

$$\theta_b\Big|_{rad} = -\frac{2\theta_I R_I}{R_E + R_I - L} \tag{4.13}$$

$$\tag{4.14}$$

then the $\theta_b\Big|_{rad}$ can be written, using Equations 4.3 4.4, as:

$$\theta_b\Big|_{rad} = \alpha\theta_I - \alpha\frac{R_E}{R_I}\theta_E \tag{4.15}$$

$$\theta_b\Big|_{rad} = 2\alpha\theta_I = -\frac{2\theta_I R_I}{R_E + R_I - L} \tag{4.16}$$

thus:

$$\alpha = -\frac{R_I}{R_I + R_E - L} = 11.91 \tag{4.17}$$

obtaining a calibrated matrix equal to:

$$\begin{pmatrix} \theta_b\Big|_{rad} \\ x_b\Big|_{mm} \end{pmatrix} = \begin{pmatrix} 11.91 & -11.91\frac{R_E}{R_I} \\ 0.71 & 0.71\frac{R_E}{R_I} \end{pmatrix} \cdot \begin{pmatrix} \theta_I \\ \theta_E \end{pmatrix}$$
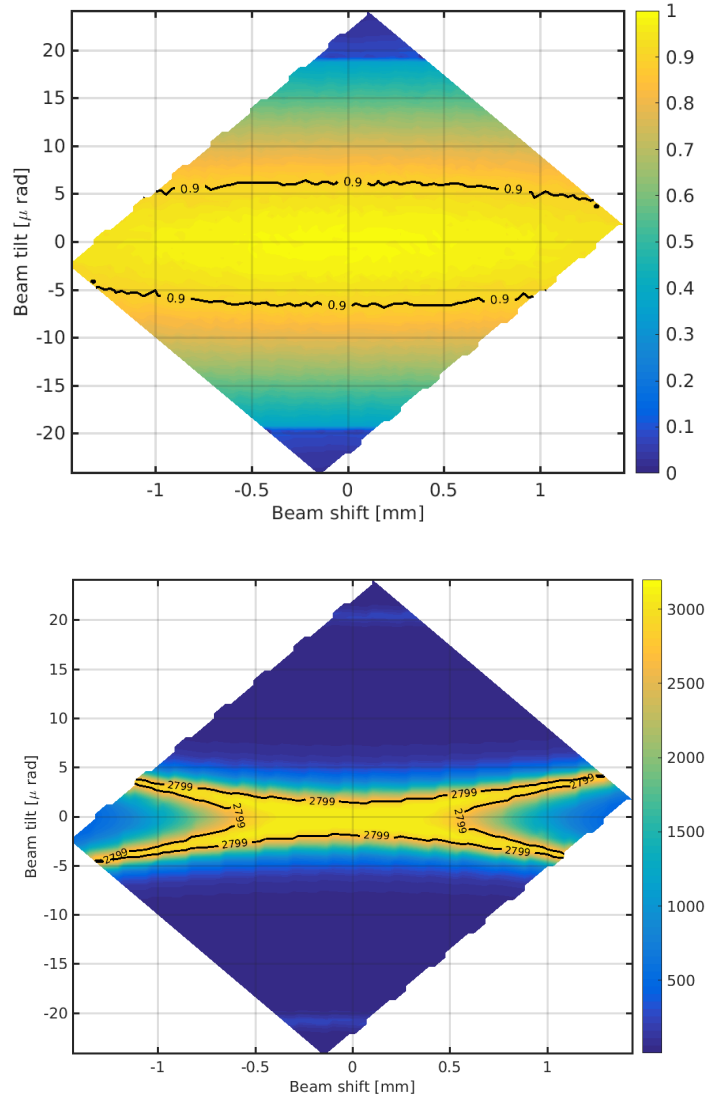
Figure 15: **Top plot:** 3D plot of the optical gain variation for the longitudinal error signal, the requirement is set to have an optical gain variation between 0.9 to 1 (a maximum loss of optical gain of 10%). The requirement on the beam tilt, within the locking control bandwidth, become then about 6.3 μrad. For the beam shift an increase of the scan region will be shown in the following plots. **Bottom plot:** 3D plot of the intra-cavity power as a function cavity axis misalignment. The requirement on the beam tilt, above the locking control bandwidth, is 1.6 $\mu rad/\sqrt{Hz}$. While the beam shift is 0.7 $mm/\sqrt{Hz}$.

The requirements on the beam tilt/shift basis can be seen in Figure 15. The problem on the computation of the optical gain variation is that the scan region is too small for the shift dof, thus a wider scan has been performed by misaligning the mirrors in such a way to obtain a pure tilt and a pure shift and the result is shown in the following plots, see Figure 16.
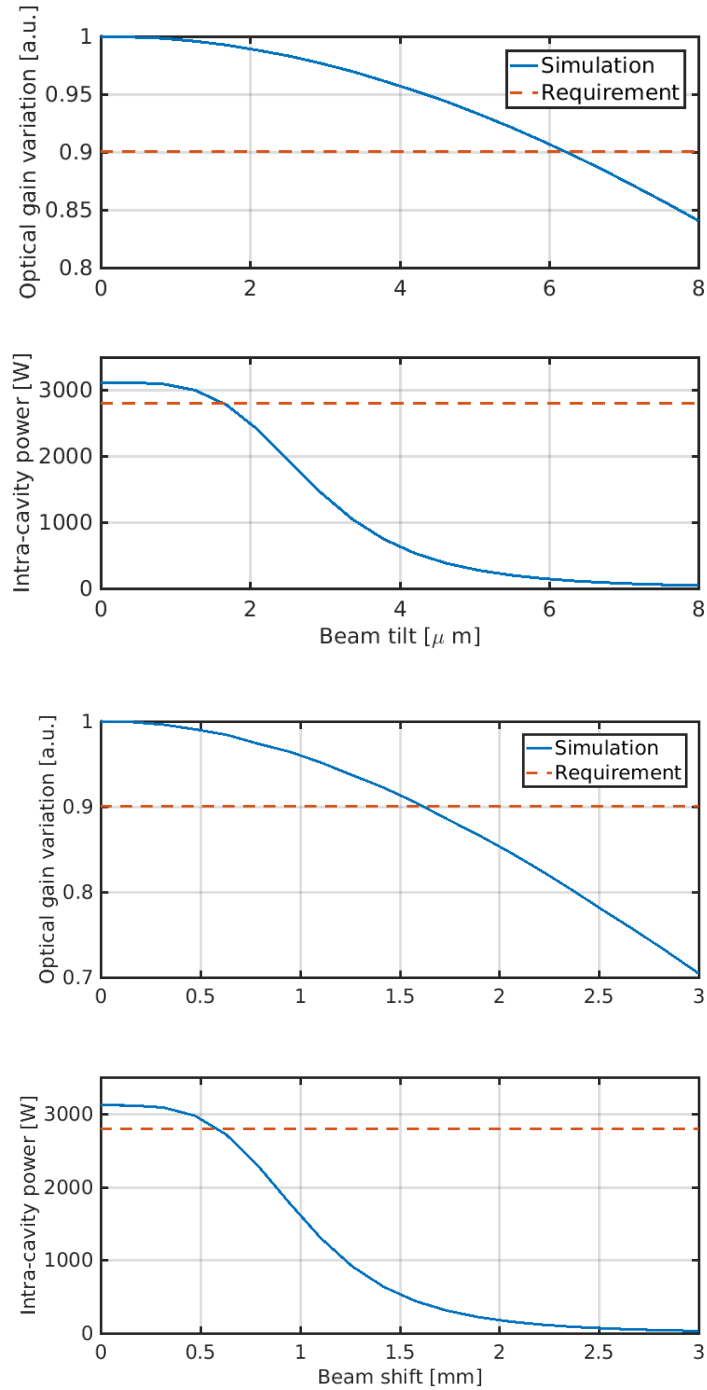
Figure 16: **Top plots:** 2D plots of the beam tilt requirements. On the first the requirement in the loop bandwidth is shown, the one which ensure a maximum optical gain variation of a factor 10%, which is 6.3 μrad. In the plot just below it the requirement above the loop u.g.f. is shown and corresponds to 1.7 $\mu rad/\sqrt{Hz}$. **Bottom plots:** 2D plots of the beam shift requirements. On the first the requirement in the loop bandwidth is 1.6 mm and above the loop u.g.f., the very last plot, is 0.7 $mm/\sqrt{Hz}$.

The requirements for the beam tilt and shift, shown in Figure 16, can be summarized in the following table:

DOF	Frequency region	Requirement value
tilt (θ_b)	below Arm lock UGF	6.3 $[\mu rad$ ToTrms]
tilt (θ_b)	above Arm lock UGF	1.7 $[\mu rad/\sqrt{Hz}]$
shift (x_b)	below Arm lock UGF	1.6 $[mm$ ToTrms]
shift (x_b)	above Arm lock UGF	0.7 $[mm/\sqrt{Hz}]$

Table 3: Angular displacement requirements for the Advanced Virgo+ green beam dofs.

The requirement, displayed in Table 3.

5   Conclusion

In this Virgo note the computation for the alignment requirement on the cavity mirrors and the green beam jitter is described. The requirements have been computed differently depending if the mirror/beam misalignment occurs within or above the longitudinal control bandwidth and it can be summarized, using the Tables 2 3, in the following table:

DOF	Frequency region	Requirement value
mirror mis. (θ_M)	f < Arm lock UGF	0.41 $[\mu rad$ ToTrms]
mirror mis. (θ_M)	f > Arm lock UGF	0.099 $[\mu rad/\sqrt{Hz}]$
beam tilt (θ_b)	f < Arm lock UGF	6.3 $[\mu rad$ ToTrms]
beam tilt (θ_b)	f > Arm lock UGF	1.7 $[\mu rad/\sqrt{Hz}]$
beam shift (x_b)	f < Arm lock UGF	1.6 $[mm$ ToTrms]
beam shift (x_b)	f > Arm lock UGF	0.7 $[mm/\sqrt{Hz}]$

Table 4: Angular displacement requirements for the Advanced Virgo+ cavity mirrors using green beam.

From these requirements it is clear that a Drift control has to be implemented [10], which has proven to provide a control accuracy of few tenths of μrad, for the mirror angular control and a beam pointing control [7] for the injected green beam.
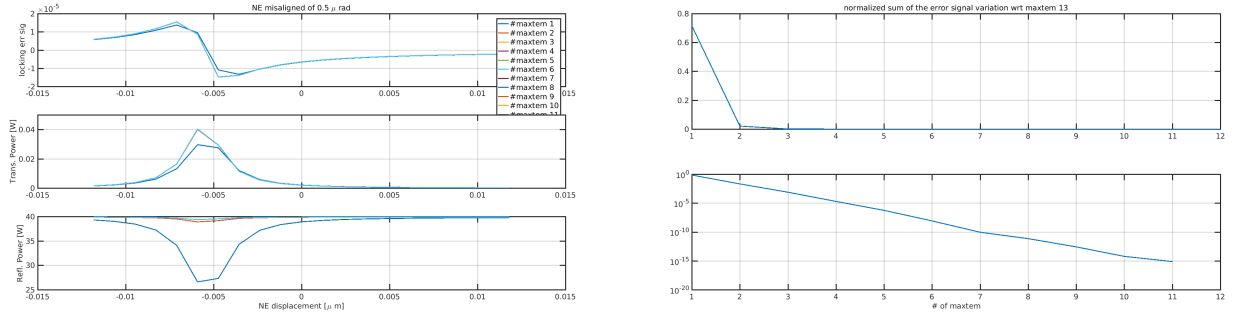
A Convergence analysis

Figure 17: **Left picture:** Comparison between cavity scans, having the End mirror misaligned of 0.5 μrad, with different maxtem values, i.e. the number of HOMs taken into account in the simulation. This analysis will give a lower limit on the number of HOMs to be used to have reliable results. **Right picture:** Normalized integral of the absolute value of the longitudinal error signal variation with respect the maxtem 13. The system converges quite quickly for maxtem larger than 3, as expected since it is a stable cavity.

The first task for the reliability of the simulation is the convergence analysis. This is needed since Finesse is a modal simulation and the minimum number of HOMs to be used has to be simulated in order to have reliable results. Of course since the long arm cavity for Advanced Virgo and Advanced Virgo+ is a stable cavity, an high number of HOMs to get the convergence of the results is not expected.

The test simulation to be tested has been chosen to be a simple scan of the cavity length and an error signal in transmission to the cavity has been chosen. It is visible from Figures 17 that the simulation converges for maxtem larger than 3, thus to be safe maxtem equal to 5 has been used for the simulations.

B Angular requirements for YAG laser

In order to cross check the simulation outcomes, the same analysis has been performed for the Advanced Virgo cavity, using the YAG beam. As it is expected from computation the requirements for the optical gain variation should be more stringent for the Green with respect for the YAG of a factor $\sqrt{2}$ and the requirement for the optical path length should be a at maximum a factor $\sim$1.18 more relaxed for the Green. Above the locking U.G.F. it is not trivial to foreseen the difference in requirements between the two cavities since in that region, even if the optical path length variation is the dominant effect, both of the two mechanisms play a role, the generation of HOMs and the optical path length variation.

B.1 Arm cavity locking

In this case the error signal used for the locking is the one actually implemented in Advanced Virgo, the B8 demodulated at 6MHz see Figure 18, which is taken in transmission from the cavity, since the injection of the beam occurs at the input mirror.
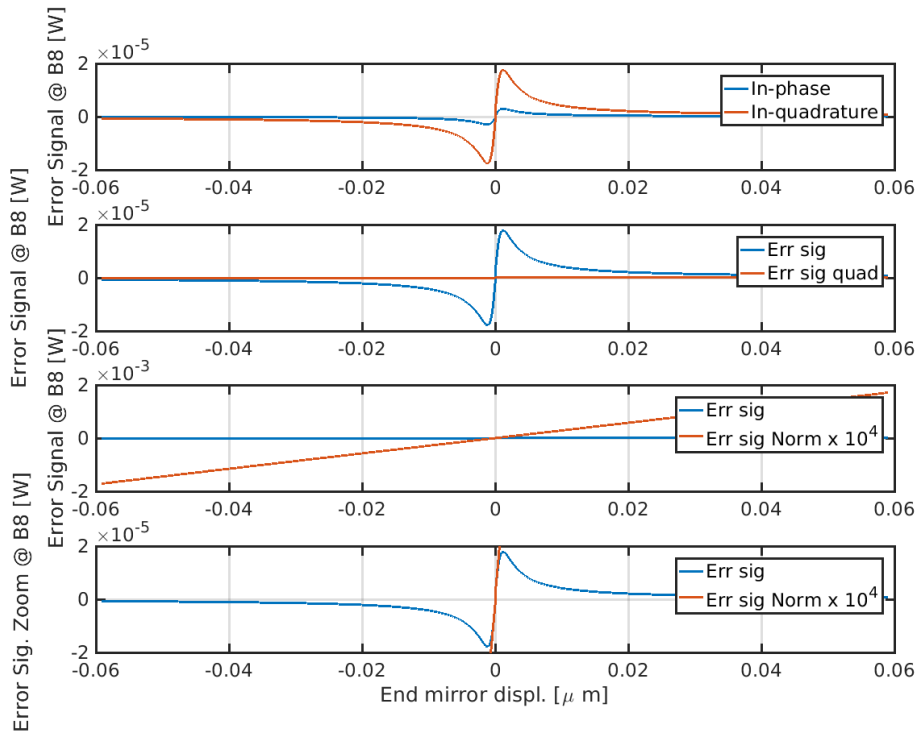
Figure 18: *1st plot from the top:* The in-phase and quadrature signal of the transmitted beam (B8), blue and red curve respectively. *2nd plot:* The error signal, having the demodulation phase tuned blue curve, and its quadrature, red curve. *3rd plot:* Comparison between the error signal and the normalized signal, on the intra-cavity power. It is visible that using the normalized error signal the linear region become very wide. *4th plot:* Zoom of the comparison between the error signal and the normalized signal, on the intra-cavity power.

The cavity scan can be zoomed to highlight the region in which the power stays above the 0.9 threshold on the maximum intra-cavity power, see Figure 19.
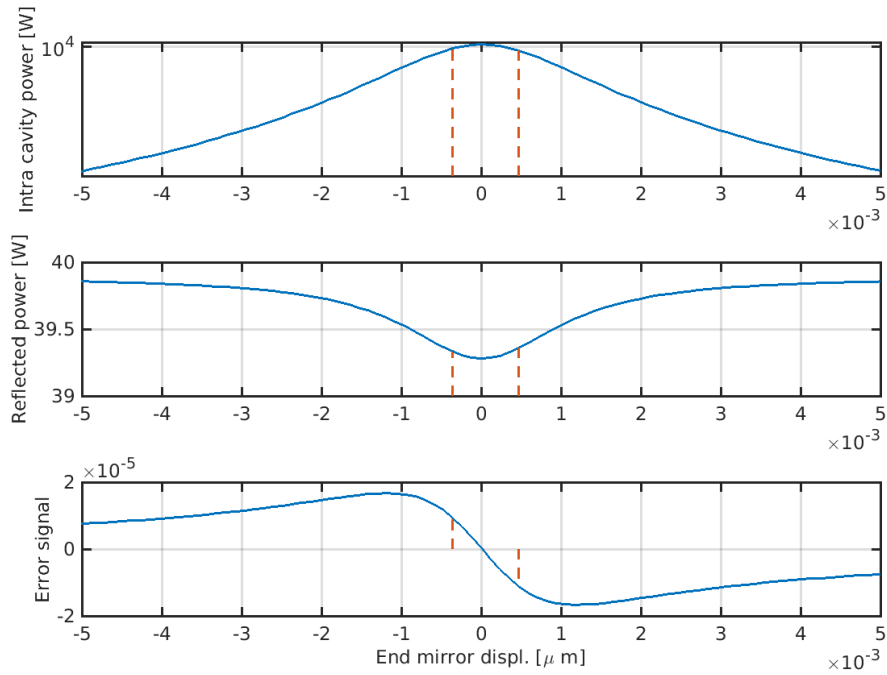
Figure 19: *Top plot:* Scan of the intra-cavity power as a function of the End mirror displacement. The dashed red lines highlight the safety region, for which the requirements have been set. The minimum allowable power drop corresponds then to have an intra-cavity power of 9379 W (a loss of 10%. *Middle plot:* Scan of the reflected power. *Bottom plot:* Scan of the locking error signal as a function of the End mirror displacement, on which the requirement has been computed.The safety region corresponds to $\pm 3.546 \cdot 10^{-4} \mu m$.

The requirement on the maximum allowable power drop has been set then to be of about 10% equal to 9.4kW circulating in the long arm.

B.2   Requirements on the YAG cavity

The 2d scan on the mirror misalignments has been performed for the Advanced Virgo cavity using YAG beam.
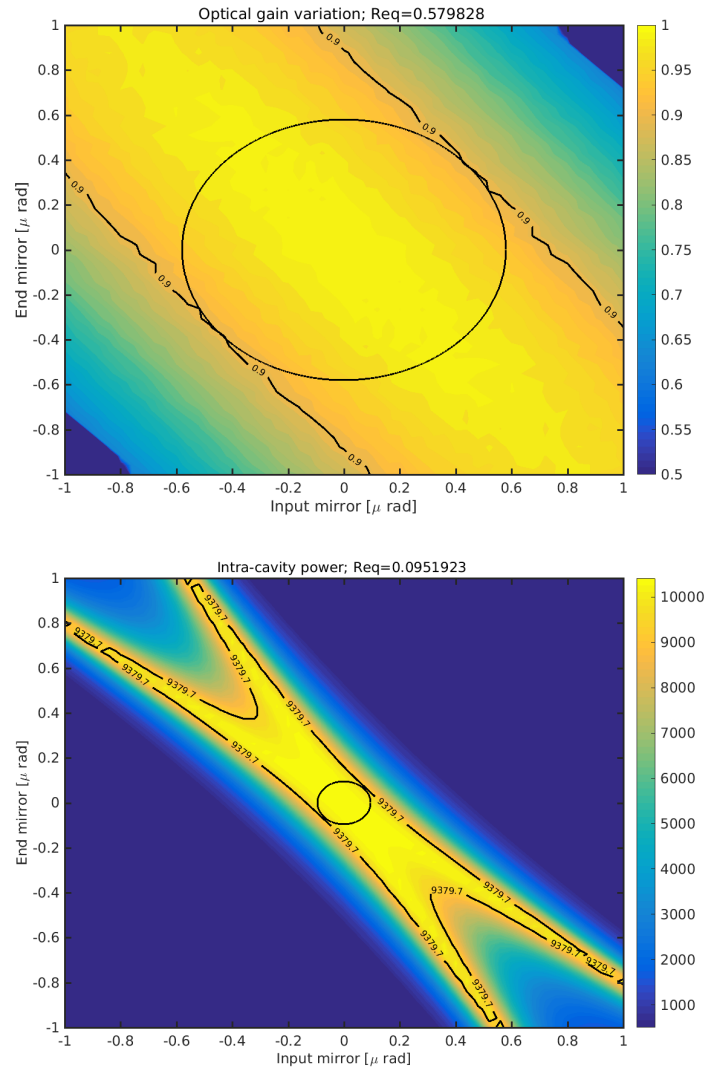
Figure 20: **Top Plot:** 3D plot of the optical gain variation for the longitudinal error signal, the requirement is set to have an optical gain variation between 0.9 to 1. The requirement on the mirrors misalignment, within the locking control bandwidth, become then 0.6 $\mu rad\ ToT_{RMS}$, which corresponds to the Green requirement relaxed by a factor $\sqrt{2}$. **Bottom Plot:** 3D plot of the intra-cavity power as a function cavity axis misalignment. The requirement on the mirror misalignment, above the locking control bandwidth, is 0.95 $\mu rad/\sqrt{Hz}$.

The requirement within the locking U.G.F. is a factor $\sqrt{2}$ more relaxed with respect to the green while the requirement above the locking U.G.F. is slightly more stringent than the Green one, see Figure 20, as expected.
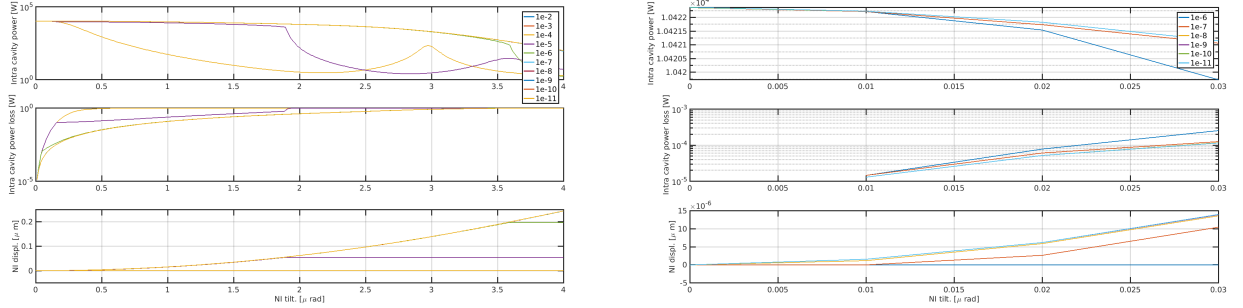
C Locking accuracy

Figure 21: **Left picture:** Comparison of the intra-cavity power, while the Input mirror misalignment is scanned, for different locking accuracy. The simulation results start to converge for a Finesse locking accuracy larger than 10^-7a.u. For safety the standard locking accuracy used for the whole analysis has been chosen to be 1 ndeg. **Right picture:** Zoom in the origin to better appreciate the effect of the locking accuracy increase.

If in the simulation the *Finesse* locking is used it would be worth to compute the locking accuracy requirement is needed to have a reliable simulation outcome (suggestion to the user). In order to evaluate which is the minimum locking accuracy needed to lock the cavities the locks with increasing accuracy (from 10^{-2} deg to 10^{-11} a.u. [4]) has been compared.

From Figure 21 it is visible that the results start to be reliable for a locking accuracy larger that 10^{-7} a.u., thus in order to have a safety margin, the locking accuracy used for the entire analysis has been chosen to be 10^{-9}. It is worth to mention that for some analysis the lock in Finesse has not been implemented, to speed up the simulation time, and the locking has been faked by scanning, for each angular working point, the longitudinal position of one of the cavity mirror and take the simulation outcome at the maximum of the intra-cavity power.
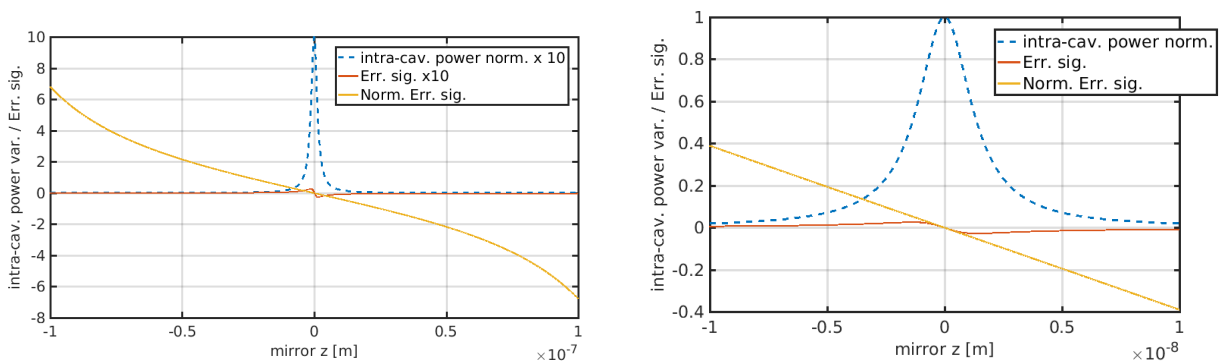
D Error signal normalization

Figure 22: **Left picture:** Comparison between the normalized error signal and the standard error signal as a function of the longitudinal position of the cavity mirror. The linear region of the normalized error signal is much wider.**Right picture:** Zoom of the scan.

---

[4]This requirement is what is written on the finesse file and it is related to the amplitude of the error signal.
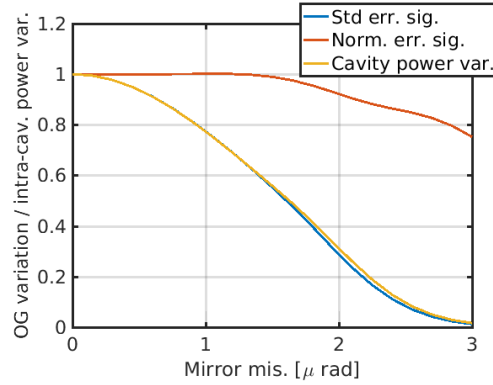
Figure 23: Beahavior of the standard error signal optical gain, blue curve, normalized error signal optical gain, red curve, and cavity power drop as a function of the cavity mirror misalignment. It is clear that the cavity recycling is completely spoiled even if the error signal optical gain, in case of the normalized one, is not affected.

In order to easier the lock acquisition time, the Pound-Drever-Hall signal can be combined with the DC signals extracted from the ITF, see Figure 22, in order to extend its linear range around the resonance [11]. This enlargement can be obtained by dividing the Pound-Drever-Hall signal by the transmitted (or intra-cavity power in case of simulation P_{incav}) from the cavity P_{tr}. In fact, in terms of the carrier power stored inside the cavity P_{incav}:

$$P_{incav} = \frac{t_1^2}{|1 - r_1 r_2 e^{i\psi_0}|^2} P_{in} \tag{D.1}$$

the error signal is [11]:

$$PDH = -2t^2 r_2 P_{incav} \frac{J_1(m)}{J_0(m)} sin(\psi_0) \tag{D.2}$$

by normalizing on the stored power:

$$PDH_{norm} = -2t^2 r_2 P_{incav} \frac{J_1(m)}{J_0(m)} sin(\psi_0) \tag{D.3}$$

$$PDH_{norm} = -2t^2 r_2 P_{incav} \frac{J_1(m)}{J_0(m)} sin\left(\frac{2\Delta L\omega_0}{c}\right) \tag{D.4}$$

$$\tag{D.5}$$

having a linear region of:

$$\Delta L < \frac{\lambda}{4\pi} \tag{D.6}$$

Of course the normalization helps in maintaining the lock but not in keeping good recycling of the cavity power, see Figure 23. The requirements have to be set then in narrower region in order to keep a good recycling.

E   Finesse script for the WE cavity

```
%%% FTblock Laser
# The input power for O4
l i1 40 0 0 nin
s s0 1m nin nEOM1a
%%% FTend Laser

%%% FTblock EOMs
# modulation frequencies
const fg 37000              # 37kHz
mod EOM1 $fg 0.15 1 pm 0 nEOM1a nEOM1b
%%% FTend EOMs

%%% FTblock Narm
s sSWEB 0.2 nEOM1b nWE1

m2 WEAR $R_WEAR $L_WEAR $WEAR_phi nWE1 nWEsub1
s sWEsub .2 $nsilica nWEsub1 nWEsub2
m1 WE $T_WE $L_WE $WE_phi nWEsub2 nWE2

s LN 2999.8 nWE2 nWI1

m1 WI $T_WI $L_WI $WI_phi nWI1 nWIsub1
s sWIsub .2 $nsilica nWIsub1 nWIsub2
m2 WIAR $R_WIAR $L_WIAR 0 nWIsub2 nWI2
%%% FTend Narm

%%% FTblock Gaussian
# Arm
cav cavW WE nWE2 WI nWI1
maxtem 5
%%% FTend Gaussian

%%% FTblock ROCs # HR-surfaces
attr WI Rc 1424.6      # Measured cold IFO WI RoC [VIR-0544A-14]
attr WE Rc -1695         # Measured cold IFO WE RoC [VIR-0269A-15]
# AR-surfaces
attr WIAR Rc 1424.6      # Approximately the same as measured HR surface
%%% FTend ROCs

%%% FTblock RTLs for Green
# Specifying reflectivities, transmissions, and losses.
 const T_WE    0.022
 const T_WI    0.0101
# Losses
const L_WE     0.24e-6
const L_WI 0.22e-6
# AR-surfaces
const R_WIAR 32u          # WI AR reflectivity [IM04, VIR-0544A-14]
const R_WEAR 32u
const L_WEAR 0
const L_WEAR 0
%%% FTend RTLs

%%% FTblock Tunings
# Tunings [deg]
const WEAR_phi 0.00
const WI_phi   0.00
const WE_phi   0.00
%%% FTend Tunings

%%% FTblock Constants
# Refractive index of silica
const nsilica 1.44963
const l_arm 2999.8         # Arm length
lambda 0.532u       # Green wavelength
%%% FTend Constants

%%% FTblock Mass
attr WI M 42
attr WE M 42
%%% FTend Mass

%%% FTblock Powers
# Input power to the Cavity
pd P_in nWE2
ad Ad_in 0 nWE2  # carrier content
# Arms, intra cavity power
pd P_INCAV nWE2
%%% FTend Powers

%%% FTblock Errsigs
pd1 errB8_g $fg 91 nWE2
pd1 errB8_gof $fg -1 nWE2
%%% FTend Errsigs

%%% FTblock Lock
set Armerr errB8_g re
lock Armz $Armerr  -100    0.00000001u
# send feedback to mirrors, adding to pre-set operating point
put* WI phi $Armz
put* WIAR phi $Armz
%%% FTend Lock
```

References

[1] Virgo Collaboration, "The Advanced Virgo longitudinal control system for the O2 observing run" accepted by Astroparticle Physics 2

[2] J. Casanueva, N. Leroy "Auxiliary Laser system: study of the lock acquisition strategy", Internal Virgo Note VIR-0327A-19 2

[3] The Virgo collaboration "Advanced Virgo Plus Phase I - Design Report" VIR-0596A-19 2

[4] M. Mantovani, E. Calloni "Radiation pressure effect on the Advanced Virgo Plano-Concave configuration'" VIR-0161A-10 https://tds.virgo-gw.eu/ql/?c=7294 5

[5] Virgo Collaboration, 'Advanced Virgo Technical Design Report' - VIR-0128A-12 6

[6] M. Mantovani "ISC for AdV+ : Status and plans" - presentation at the Virgo Week (Advanced Virgo + session) on the 5th of November 2019. VIR-1112A-19 https://tds.virgo-gw.eu/ql/?c=14946. A Virgo note is in preparation (M. Valentini) 7

[7] B. Canuel, E. Genin, M. Mantovani, J. Marque, P. Ruggi, and M. Tacca "Sub-nanoradiant beam pointing monitoring and stabilization system for controlling input beam jitter in gravitational wave interferometers", Applied Optics Vol. 53, Issue 13, pp. 2906-2916 (2014) https://doi.org/10.1364/AO.53.002906 7, 19

[8] A. Freise et al, "Frequency domain interferometer simulation with higher-order spatial modes", Class. Quant. Grav. 2005 vol 21 n 5 7

[9] J. Casanueva "Control of the gravitational wave interferometric detector Advanced Virgo" PhD thesis VIR-0878A-17 14

[10] T. Accadia, et al. "Automatic Alignment system during the second science run of the Virgo interferometer", Astroparticle Physics Volume 34 (2011) 327-332 19

[11] L. Barsotti Phd thesis "The control of the Virgo interferometer for gravitational wave detection" Universita Pisa 25